MODELING ALASKA BOREAL FORESTS WITH A CONTROLLED TREND SURFACE APPROACH[a]

Mo Zhou and Jingjing Liang*

ABSTRACT

An approach of Controlled Trend Surface was proposed to simultaneously take into consideration large-scale spatial trends and nonspatial effects. A geospatial model of the Alaska boreal forest was developed from 446 permanent sample plots, which addressed large-scale spatial trends in recruitment, diameter growth, and mortality. The model was tested on two sets of validation plots and the results suggest that the controlled trend surface model was generally more accurate than both nonspatial and conventional trend surface models. With this model, we mapped the forest dynamics of the entire Alaska boreal region by aggregating predicted stand states across the region.

INTRODUCTION

Geospatial effects at large scales have been reported in many biological and ecological studies. The conventional trend surface analysis (e.g. Kuuluvainen and Sprugel 1996; Thomson 1986) has been developed to capture such trends in various disciplines (Gittins 1968) and there exist numerous studies attempting to explain these effects (e.g. Kuuluvainen and Sprugel 1996; Wilmking and Juday 2005).

Existing spatial studies of forest dynamics have been mainly focusing on small-scale spatial effects, such as interactions of neighboring trees or stands (e.g. Franklin and others 1985; Larson and others 2006; Liu and Ashton 1998; Pacala and others 1996). Little has been done to identify large-scale spatial factors of forest dynamics and separate them from small-scale variations attributable to local effects (Schenk 1996), such as site and stand basal area (e.g. Bonan and Shugart 1989; Liang and others 2005).

The purpose of this paper was to propose an innovative method, controlled trend surface (CTS), to account for both large-scale spatial effects and well-recognized nonspatial factors in modeling. With this proposed method, a geospatial dynamics model of the Alaska boreal forest was developed based on the same data that were used to calibrate the nonspatial model of Liang (2010). With remote sensing data and the Geographic Information System (GIS), stand-level predictions were aggregated to tentatively map forest dynamics of the entire region.

The Alaska boreal forest is generally defined as a biome characterized by coniferous forests. In this study, it represented a vast area composed of the following ecoregions: Interior Alaska-Yukon lowland Taiga, Cook Inlet Taiga, and Copper Plateau Taiga. Forestry is very important for the state of Alaska (AlaskaDNR 2006; Wurtz and others 2006), and is an indispensable component of rural economies (AlaskaDNR 2006). Liang (2010) develops the first Matrix Model for all major Alaska boreal tree species which is tested to be much more accurate than the two growth and yield tables. However, due to a lack of control for large-scale spatial patterns which "may cause substantial errors between actual and predicted stand states" (See Liang 2010, P.10), caution is advised when applying the Matrix Model on stands out of the sample area or on areas of considerable sizes.

METHODS

CONTROLLED TREND SURFACE (CTS)

The conventional trend surface analysis studies the spatial trend of given observations $Z(\mathbf{s})$ at location $\mathbf{s}$ within the region D (Grant 1957; Ripley 1981; Watson 1971):

$$Z(\mathbf{s})=\mu(\mathbf{s})+\delta, \qquad \mathbf{s}=(\mathbf{x},\mathbf{y})'\in\mathbf{D}\subset\mathrm{IR}^2 \tag{1}$$

where

$$\mu(\mathbf{s})=\sum_{i=1}^{k} f_{i-1}(\mathbf{s})\rho_{i-1}$$

represents an unknown linear combination of known functions $f_i(\mathbf{s})$ of spatial coordinates $\mathbf{x}=(x_1, \ldots, x_n)'$ and $\mathbf{y}=(y_1, \ldots, y_n)'$ with unknown but fixed parameters ρ_i, $i=1,2,\ldots,k$-1. δ is a zero-mean, stationary error term with known covariogram (see Berke 1999, p.219).

Mo Zhou, School of Management, University of Alaska Fairbanks, Fairbanks, AK 99775-6080
Jingjing Liang, Department of Forest Sciences, University of Alaska Fairbanks, P.O.Box 757200, Fairbanks, AK 99775-7200, USA
Tel: 907-474-1831; Fax: 907-474-6184; Email: jliang@alaska.edu
[a] This paper is condensed and modified from Liang and Zhou (2010).
*Corresponding author.

Now assume that δ was controlled by non-spatial factors **n**, viz. the factors with distributions independent from location **s**=(**x**,**y**)', the model of controlled trend surface (CTS) was obtained as follows:

$$Z(\mathbf{s})=\mu(\mathbf{s})+\varsigma(\mathbf{n})+\zeta, \quad \mathbf{s}=(\mathbf{x},\mathbf{y})'\in\mathbf{D}\subset IR^2 \tag{2}$$

with $\varsigma(\mathbf{n})$ being the nonspatial component— an unknown combination of functions of non-spatial factors and ζ representing a zero-mean, stationary error term with known covariogram independent from both spatial and non-spatial factors. Apparently, under-parameterized conventional trend surface estimates were biased when nonspatial effects were present. In this case, CTS model (Eq. 2) was appropriate and provided unbiased estimates.

MODEL DESCRIPTION

A conventional Matrix Model (e.g. Buongiorno and others 1995; Liang and others 2005) predicts the forest stand state in Year t+1 based on the stand state in Year t:

$$\mathbf{y}_{t+1}=\mathbf{G}\mathbf{y}_t+\mathbf{R}+\varepsilon \tag{3}$$

where $\mathbf{y}_t = [y_{ijt}]$ was a column vector representing the number of live trees per unit of land area of species i and diameter class j at time t. ε was a random error. **G** and **R** represented a spatial-independent growth matrix and recruitment vector, respectively.

The CTS Matrix Model extended Eq. 3 to control for the large-scale spatial trend by recognizing geographic location and terrain characteristics of the stand:

$$\begin{aligned}&\mathbf{V}_{t+1}(\mathbf{s})=\mathbf{G}(\mathbf{s})\mathbf{V}_t(\mathbf{s})+\mathbf{R}(\mathbf{s})+\varepsilon\\&\mathbf{s}=(\mathbf{x},\mathbf{y})'\in\mathbf{D}\subset IR^2\end{aligned} \tag{4}$$

where $\boldsymbol{V}_t(s)=[v_{ijt}(s)]$ was a space-dependent column vector representing the number of live trees per unit of land area of species i (i=1,…,4) and diameter class j (j=1,…,19) at location **s** and at time t. ε was a zero-mean, stationary process with known covariogram. **x** and **y** represented the plot coordinates within the Alaska boreal forest region D in the plane (IR^2).

G(**s**) was a state- and space-dependent matrix that described how trees grew or died between t and t+1 at location **s**. **R**(**s**) was a state- and space-dependent vector representing the recruitment of each species between t and t+1 at location **s**.

The **G**(**s**) and **R**(**s**) matrices were defined as:

$$\mathbf{G}(\mathbf{s})=\begin{bmatrix}\mathbf{G}_1(\mathbf{s}) & & & \\ & \mathbf{G}_2(\mathbf{s}) & & \\ & & \ddots & \\ & & & \mathbf{G}_m(\mathbf{s})\end{bmatrix},\ \mathbf{G}_i(\mathbf{s})=\begin{bmatrix}a_{i1}(\mathbf{s}) & & & & \\ b_{i1}(\mathbf{s}) & a_{i2}(\mathbf{s}) & & & \\ & \ddots & \ddots & & \\ & & b_{i,n-2}(\mathbf{s}) & a_{i,n-1}(\mathbf{s}) & \\ & & & b_{i,n-1}(\mathbf{s}) & a_{in}(\mathbf{s})\end{bmatrix} \tag{5}$$

$$\mathbf{R}(\mathbf{s})=\begin{bmatrix}\mathbf{R}_1(\mathbf{s})\\ \mathbf{R}_2(\mathbf{s})\\ \vdots\\ \mathbf{R}_m(\mathbf{s})\end{bmatrix},\ \mathbf{R}_i(\mathbf{s})=\begin{bmatrix}R_i(\mathbf{s})\\ 0\\ \vdots\\ 0\end{bmatrix}$$

where $R_i(\mathbf{s})$ was the number of trees of species i recruited in the smallest diameter class (3.8cm) each year at location **s**. Recruitment was zero in all the higher diameter classes. The probabilities of a tree of species i and diameter class j stayed alive in the same diameter class $a_{ij}(\mathbf{s})$, and stayed alive and move up a diameter class $b_{ij}(\mathbf{s})$ between t and t+1 at location **s** were related by:

$$a_{ij}(\mathbf{s}) = 1-b_{ij}(\mathbf{s}) - m_{ij}(\mathbf{s}) \tag{6}$$

where $m_{ij}(\mathbf{s})$ was the probability that a tree of species i and diameter class j died between t and t+1 at location **s**. $b_{ij}(\mathbf{s})$ was calculated as the annual tree diameter growth $g_{ij}(\mathbf{s})$ divided by the width of the diameter class (2 cm except for the first diameter class of 1.2 cm width), assuming that trees were evenly distributed in a diameter class.

It was assumed that the large-scale spatial trend $\mu(\mathbf{s})$ was represented by a second-order polynomial function of northing (y) and easting (x) coordinates:

$$(\mathbf{s}) = d_0 + d_1x + d_2y + d_3x^2 + d_4y^2 + d_5xy \tag{7}$$

where d's were coefficients to be estimated in each equation. Northing and easting coordinates of the Universal Transverse Mercator system (UTM, see Snyder 1987) were used here to approximate the Cartesian system in which the distance between permanent sample plots could be easily calculated (Ripley 1981). The easting values were then set as the absolute distance from the center of that UTM zone to mitigate edge effects near borders.

The non-spatial component of the recruitment, $R_i(\mathbf{s})$, diameter growth $g_{ij}(\mathbf{s})$, and mortality $m_{ij}(\mathbf{s})$ was composed of a terrain function and stand basal area (B), permafrost(P), and the number of tree species present in the plot(H), as B and P have been employed as key predictors in many existing forest dynamics models (e.g. Boltz and Carter 2006;

Bonan and Shugart 1989; Liang and others 2005; Namaalwa and others 2005), and *H* represented marked differences in species life histories with effects of complementarity and niche facilitation that may change forest dynamics(Liang and others 2007). In addition, D_j, the midpoint of the DBH class *j*, was used in both diameter growth and mortality equations, as tree size is an important factor of diameter growth and mortality (Buongiorno and Michie 1980; Buongiorno and others 1995; Liang and others 2005). Stem density, the number of trees per hectare of the species of interest (*N*), was used in recruitment equation to represent the abundance of seeds and seedlings (Liang and others 2005; Liang and others 2007). Although the presence of permafrost (*P*) was significantly correlated with the northing (ρ=0.18, *p*-value=0.00), since the correlation coefficient was small and the effect of permafrost on forest growth is local (Chapin and others 2006), permafrost(*P*) was considered as a non-spatial variable. None of the other non-spatial variables was spatially correlated.

The terrain component (Eq. 8) represented the interacting effects of the slope (l), aspect (α), and elevation (z) on site productivity (see Stage and Salas(2007), p.487). The function has been tested a better proxy of site productivity than other existing terrain functions, and is considered as an inseparable entity, in which all the terms are conjoint and should be used together or not at all (Stage and Salas 2007).

$$\tau(l,a,z) = c_0 + l[c_1 + c_2\cos(a) + c_3\sin(a)] + \ln(z+1)\cdot l[c_4 + c_5\cos(a) + c_6\sin(a)] + z^2\cdot l[c_7 + c_8\cos(a) + c_9\sin(a)] + c_{10}z + c_{11}z^2 \quad (8)$$

where *c*'s were parameters to be estimated in each equation.

The annual diameter growth $g_{ij}(\mathbf{s})$ was estimated by the following model:

$$g_{ij}(\mathbf{s}) = \gamma_0 + \gamma_1 D + \gamma_2 D^2 + \gamma_3 D^3 + \gamma_4 B + \gamma_5 P + \gamma_6 H + \tau(l,a,z) + \mu(\mathbf{s}) + \varepsilon_1 \quad (9)$$

where γ's were parameters to be estimated , and ε_1 was a random error independent of spatial patterns.

The probability of annual mortality rate, $m_{ij}(\mathbf{s})$, was calculated by dividing $M_{ij}(\mathbf{s})$ by the elapsed time of *T* years between the two inventories. $M_{ij}(\mathbf{s})$=1 if a tree died between the two inventories, and $M_{ij}(\mathbf{s})$=0 otherwise. $M_{ij}(\mathbf{s})$ was estimated with a species- and size-dependent Probit function (Bliss 1935):

$$M_{ij}(\mathbf{s}) = \Phi(\delta_0 + \delta_1 D + \delta_2 D^2 + \delta_3 D^3 + \delta_4 B + \delta_5 P + \delta_6 H + \tau(l,a,z) + \mu(\mathbf{s})) + \varepsilon_2 \quad (10)$$

where Φ was the standard normal cumulative function, and δ's were parameters and ε_2 was a random error independent of spatial patterns.

The expected recruitment of species *i* was estimated with the following model:

$$R_i(\mathbf{s}) = \beta_0 + \beta_1 N_i + \beta_2 B + \beta_3 P + \beta_4 H + \tau(l,a,z) + \mu(\mathbf{s}) + \varepsilon_3 \quad (11)$$

where β's were the parameters, and ε_3 was a random error independent of spatial patterns.

DATA

The CTS Matrix Model presented here was calibrated with data from 446 remeasured permanent sample plots of the Cooperative Alaska Forest Inventory (CAFI) (Malone and others 2009). The sample area stretches over 500km from the Kenai Peninsula in the south to the Fairbanks area in the north, and represents a wide range of stand conditions and species composition (Fig. 1). The same data, except for geographic coordinates, have been used to calibrate the nonspatial Matrix Model of Liang (2010) (Table 1).

The species studied here were *Betula neoalaskana* Sarg. (birch), *Populus tremuloides* Michx. (aspen), *Picea glauca* (Moench) Voss (white spruce), and *Picea mariana* (Mill.) B.S.P. (black spruce). White spruce had the highest basal area of all the species (37 percent), followed by birch (28 percent), aspen (20 percent), and black spruce (5 percent). The other species, *Populus trichocarpa* Torr. &Gray*, P. balsamifera* L. *Larix laricina* (DuRoi) K.Koch, and *Betula kenaica* W.H. Evans, accounted for less than 10 percent of the total basal area (Table 2). Trees were grouped into 19 diameter classes by species, from 3.8 to 5.0 cm up to 39.0 cm and above. Tables 3 and 4 display the summary statistics of plot level and individual tree variables.

PARAMETER ESTIMATION AND MODEL VALIDATION

The recruitment $R_i(\mathbf{s})$ and diameter growth $g_{ij}(\mathbf{s})$ equations were estimated by the generalized least squares (GLS) method (Rao 1973), and a generalized coefficient of determination (Nagelkerke 1991) was calculated for each equation as a proxy for the common coefficient of determination. Mortality $m_{ij}(\mathbf{s})$ was a Probit function (Bliss 1935) estimated with maximum likelihood.

To avoid compromised type-I error rates and severe artifacts commonly associated with model selection procedures (Mac Nally 2000), predictive variables were selected with three criteria: the expected biological responses, the statistical significance, and the contribution to the model goodness-of-fit. In this study, we used the hierarchical partitioning or HP (Chevan and Sutherland 1991) to decompose the model goodness-of-fit represented by likelihood through incremental partitioning, and determined the average independent contribution of each variable to the overall goodness-of-fit. The HP analysis was conducted with the

hier.part package of the R program (Mac Nally and Walsh 2004).

The accuracy of this model was determined by the prediction errors, the differences between the observed stand states of the third inventory and the predicted ones, on two phases of validation plots. Phase I plots were 175 CAFI sample plots on which a third inventory has been conducted 10 years after the first inventory, solely for the validation purpose. Phase II was consisted of 40 Forest Inventory and Analysis (FIA) plots located on the boreal transitional zone on the Kenai Peninsula outside the current sample area, and no data from these plots were used to calibrate the CTS model. Phase I and II plots represented a temporal and spatial extension of the current sample coverage, respectively (Fig. 1). For each Phase I plot, the expected number of trees at the third inventory was predicted by setting the stand state at the first inventory as the initial state, and applying Eq. 4 iteratively over 10 years. For each Phase II plot, the expected number of trees at the second inventory was predicted by applying Eq. 4 iteratively over the specific interval of that plot, averaging 4.78 years across all the plots.

For comparison, we also predicted the stand states of both Phase I and II plots with the nonspatial Matrix Model (Liang 2010) and a conventional trend surface Matrix Model in which recruitment, diameter growth, and mortality were equations of second-order trend surfaces only (Eq. 7). Both models were calibrated with data from the same 446 sample plots. For each model, root mean squared errors (RMSE, see Wooldridge 2000, P.600) were calculated based on the difference between the predicted and observed basal area by diameter class and species as a measure of accuracy of that model over the validation plots.

RESULTS

MODEL PARAMETERS

For recruitment $R_i(\mathbf{s})$, the total number of trees (N) and stand basal area (B) were the most significant control variables, and their effects on recruitment were consistent over all the species (Table 5). When regarded as an entity, the spatial component was significant for all the species in recruitment, and so was the terrain component. Generally, N contributed most to the goodness-of-fit of recruitment (67~82 percent), followed by P and H (2~14 percent). The spatial component contributed 3~9 percent, and the terrain variables 8~16 percent. B contributed little to the goodness-of-fit (2~6 percent), albeit its high level of significance (Table 6).

In the diameter growth model, all the control variables were significant, except basal area (B) for aspen and black spruce, permafrost (P) for birch, and species diversity (H) for birch and white spruce (Table 7). The spatial and terrain components were both highly significant (Table 6). Generally, the diameter (D) contributed the most to the overall goodness-of-fit of diameter growth (4~71 percent), followed by the terrain (12~33 percent) and spatial component (4~25 percent, Table 6).

In the mortality model, all the control variables were significant, except basal area (B) for aspen and black spruce, permafrost (P) for birch, and species diversity (H) for birch and white spruce (Table 8). Both the spatial and terrain components were highly significant (Table 6). Generally, the terrain component contributed the most to the overall goodness-of-fit of mortality (22~55 percent), followed by the diameter (3~51 percent) and spatial component (12~33 percent, Table 6).

VALIDATION AND RESIDUALS

Over the 175 Phase I validation plots, the stand basal area predicted by the CTS model was generally accurate over all species and size, as they all fell within 95 percent confidence interval of the observed ones, except for the smallest black spruce (Fig. 2). The nonspatial model was quite close to the CTS model in terms of predictions over the Phase I plots, and the conventional trend surface model underestimated aspen and overestimated black spruce in general. Compared to the nonspatial model, the CTS model was 7.88, 20.73, 22.28, and 11.00 percent more accurate in terms of RMSE for birch, aspen, white spruce, and black spruce, respectively. The CTS model was also 2.98, 18.41, 22.32, and 16.88 percent more accurate than the conventional trend surface model for the four species in terms of RMSE (Fig. 2).

The accuracy of the CTS model was more prevalent for deciduous species over the 40 Phase II validation plots. The CTS model was 21.41, 64.10, 7.24, and 3.70 percent more accurate in terms of RMSE than the nonspatial model for birch, aspen, white spruce, and black spruce, respectively. When compared with the conventional trend surface model, the CTS model was more than 60 percent more accurate for deciduous species, and 13.62 percent more accurate for white spruce. The CTS model was 7.98 percent less accurate than the conventional trend surface model for black spruce, but the difference was negligible especially for forest management purposes as most errors of the CTS model occur in the smallest diameter class (Fig. 3).

SPATIAL INFERENCE

Using the method in Liang and Zhou (2010), we created maps of the predicted future Alaska boreal forest. The map of the predicted stand basal area change in the Year 2011, 2051, and 2101 shows that without major disturbances and substantial changes of climate conditions, the total stand basal area would keep increasing over time for most of the

region (Fig. 4). The Yukon River Basin and Copper River Valley were predicted to have the best basal area growth. The Matanuska-Susitna Valley, Kuskokwim River Basin, and some sporadic areas, such as Nenana and Healy, on the contrary, would see a decline in the basal area. Overall, the stand basal area may increase in the central and eastern region, while some negative basal area change may occur in the southern and western region. The magnitude of changes over the entire region slightly increased over time. Between the year 2001, 2011, 2051, and 2101, the average annual basal area change was 0.20, 0.27 and 0.33 m^2/ha/y, respectively. The prediction implies that under current conditions, the total basal area of the Alaska boreal forest may become higher at an increasing rate for the Twenty-First Century.

Current distribution of dominant species throughout the region was predicted to remain the same until the Year 2051, and a large portion of the deciduous forests may switch to coniferous forests thereafter (Fig. 5). In the Year 2101, without major disturbances and catastrophes, more than 90 percent of the forest located between 62°N and 66°N was predicted to be coniferous, while at present, most of the coniferous forests are clustered in the Copper River Valley and the area to the southeast of Fairbanks. The Porcupine River Valley and eastern Mat-Su Valley, however, may continue to be covered by deciduous forests in a century, according to the model (Fig. 5).

CONCLUSION

This paper proposes a method of Controlled Trend Surface to simultaneously account for large-scale spatial trends and nonspatial local effects. By incorporating well-recognized nonspatial factors, CTS would be particularly useful for studying biological and ecological processes, such as forest growth and fish habitat alteration, where spatial patterns and effects of local variables were both important, and predictions were needed over areas of considerable sizes. With this method, a geospatial model of forest dynamics was developed for the Alaska boreal forest, based on a large and representative dataset which covers a wide range of forests, from lowland monospecific coniferous stands to upland uneven-aged hardwood stands. The CTS model was in general more accurate for all the species than the nonspatial model (Liang 2010) and the conventional trend surface model, both of which were calibrated with the same data, over the 175 Phase I and 40 Phase II validation plots.

The CTS model was beyond traditional stand growth models because its geospatial component represented trends of forest dynamics on a large spatial scale, likely caused by the spatial variation of temperature and precipitation and other unknown factors. Therefore, this model would be more useful than traditional stand growth models to predict forest dynamics over the entire Alaska boreal region. Although it was a bold extrapolation, of which the accuracy remained to be assessed for most locations outside the sample area, the predictions were generally consistent with previous knowledge and offered a striking illustration of the potential power of including spatial and topographic information in forest dynamics models.

LITERATURE CITED

AlaskaDNR. 2006. Alaska State Forester's Office Annual Report. Anchorage, AK: Alaska Department of Natural Resources, Division of Forestry. 70 p.

Berke O. 1999. Estimation and prediction in the spatial linear model. Water, Air, and Soil Pollution 110:215-237.

Bliss CI. 1935. The calculation of the dosage-mortality curve. Annals of Applied Biology 22:134-167.

Boltz F, and Carter DR. 2006. Multinomial logit estimation of a matrix growth model for tropical dry forests of eastern Bolivia. Canadian Journal of Forest Research 36(10):2623-2632.

Bonan GB, and Shugart HH. 1989. Environmental factors and ecological processes in boreal forests. Annual Review of Ecology and Systematics 20:1-28.

Buongiorno J, and Michie BR. 1980. A matrix model of uneven-aged forest management. Forest Science 26(4):609-625.

Buongiorno J, Peyron JL, Houllier F, and Bruciamacchie M. 1995. Growth and management of mixed-species, uneven-aged forests in the French Jura: Implications for economic returns and tree diversity. Forest Science 41(3):397-429.

Chapin FSI, Oswood MW, Cleve KV, Viereck LA, and Verbyla DL. 2006. Alaska's changing boreal forest. Chapin FSI, Oswood MW, Cleve KV, Viereck LA, and Verbyla DL, editors. Oxford: Oxford University Press.

Chevan A, and Sutherland M. 1991. Hierarchical partitioning. American Statistician 45:90-96.

Franklin J, Michaelsen J, and Strahler AH. 1985. Spatial analysis of density dependent pattern in coniferous forest stands. Plant Ecology 64(1):29-36.

Gittins R. 1968. Trend-surface analysis of ecological data. Journal of Ecology 56(3):845-869.

Grant F. 1957. A problem in the analysis of geophysical data. Geophysics 22:309-344.

Kuuluvainen T, and Sprugel DG. 1996. Examining age- and altitude-related variation in tree architecture and needle efficiency in Norway spruce using trend surface analysis. Forest Ecology and Management 88:237-247.

Larson JA, Franklin FJ, and Franklin J. 2006. Structural segregation and scales of spatial dependency in Abies amabilis forests. Journal of Vegetation Science 17(4):489-498.

Liang J. 2010. Dynamics and management of Alaska boreal forest: an all-aged multi-species Matrix growth model. Forest Ecology and Management 260(4):491-501.

Liang J, Buongiorno J, and Monserud RA. 2005. Growth and yield of all-aged douglas-fir/western hemlock stands: a Matrix model with stand diversity effects. Canadian Journal of Forest Research 35:2369-2382.

Liang J, Buongiorno J, Monserud RA, Kruger EL, and Zhou M. 2007. Effects of diversity of tree species and size on forest basal area growth, recruitment, and mortality. Forest Ecology and Management 243:116-127.

Liu J, and Ashton PS. 1998. FORMOSAIC: an individual-based spatially explicit model for simulating forest dynamics in landscape mosaics. Ecological Modelling 106:177-200.

Mac Nally R. 2000. Regression and model-building in conservation biology, biogeography and ecology: The distinction between – and reconciliation of – 'predictive' and 'explanatory' models. Biodiversity and Conservation 9 (5):655-671.

Mac Nally R, and Walsh C. 2004. Hierarchical partitioning public-domain software. Biodiversity Conservation 13:659-660.

Malone T, Liang J, and Packee. EC. 2009. Cooperative Alaska Forest Inventory. Portland, OR: Gen. Tech. Rep. PNW-GTR-785, USDA Forest Service, Pacific Northwest Research Station. 42 p.

Nagelkerke N. 1991. A note on a general definition of the coefficient of determination. Biometrika 78(3):691-692.

Namaalwa J, Eid T, and Sankhayan P. 2005. A multi-species density-dependent matrix growth model for the dry woodlands of Uganda. Forest Ecology and Management 213:312-327.

Pacala SW, Canham CD, Saponara J, Silander JA, Kobe RK, and Ribbens E. 1996. Forest models defined by field measurements: estimation, error analysis and dynamics. Ecological Monographs 66:1-43.

Rao CR. 1973. Linear statistical inference and its applications. New York: John Wiley. 626 p.

Ripley BD. 1981. Spatial statistics. Hoboken, NJ. : John Wiley & Sons, Inc. . 252 p.

Schenk HJ. 1996. Modeling the effects of temperature on growth and persistence of tree species: A critical review of tree population models. Ecological Modelling 92:1-32.

Snyder JP. 1987. Map projections - a working manual. U.S. Geological Survey Professional Paper ed. Washington, D.C. : United States Government Printing Office. p 385.

Stage AR, and Salas C. 2007. Interaction of elevation, aspect, and slope in models of forest species composition and productivity. Forest Science 53(4):486-492.

Thomson AJ. 1986. Trend surface analysis of spatial patterns of tree size, microsite effects, and competitive stress. Canadian Journal of Forest Research 16:279-282.

Watson GS. 1971. Trend surface analysis. Mathematical Geology 3:215-226.

Wilmking M, and Juday GP. 2005. Longitudinal variation of radial growth at Alaska's northern treeline-recent changes and possible scenarios for the 21st century. Global and Planetary Change 47:282-300.

Wooldridge JM. 2000. Introductory econometrics: a modern approach. Cincinnati, OH: South-Western College Publishing.

Wurtz TL, Ott RA, and Maisch JC. 2006. Timber harvest in interior Alaska. In: Chapin FS, Oswood MW, Van Cleve K, Viereck LA, and Verbyla DL, editors. Alaska's changing boreal forest. New York, NY: Oxford University Press. p 302-308.

Table 1—Definition of variables

Variable	Definition
Tree-level variables	
D	Diameter at breast height (cm) of a live tree
g	Annual diameter increment (cm) of a live tree
Plot-level variables	
R_i	Annual recruitment, the number of trees grew into the smallest diameter class (3.8 to 5.0 cm) of species i in a year
N_i	Total number of trees per hectare of species i
B	Stand basal area (m^2/ha)
P	Permafrost. A coded variable representing the likelihood of permafrost on site, where one stands for 90% likely, two 60% likely, three 30% likely, and four most unlikely (0%)
H	Number of tree species present on a plot
z	Plot elevation (km)
I	Plot slope (%)
α	Plot aspect showing the direction to which the plot slope faces (°). 0 means no slope, 180 and 360 represented south- and north-facing slopes, respectively.
x	Easting of UTM coordinates (10^6m)
y	Northing of UTM coordinates (10^6m)

Table 2—Distribution of total basal area by species in the sample plots

Common Name	Shortened Name	Scientific Name		Percentage
white spruce	white spruce	*Picea glauca (Moench) Voss*		37.40
Alaska birch	birch	*Betula neoalaskana Sarg.*		27.83
quaking aspen	aspen	*Populus tremuloides Michx.*		20.27
black spruce	black spruce	*Picea mariana (Mill.) B.S.P.*		4.99
Other species				9.51
			Total	100.00

Table 3—Summary statistics of plot-level variables, based on 446 sample plots

	N (trees∗ha^{-1})				*B* (m^2 ha^{-1})	*P*	*H*
	Birch	Aspen	White spruce	Black spruce			
Mean	336.35	286.82	651.20	281.56	22.91	3.33	2.32
S.D.	31.73	32.13	44.36	51.69	0.49	0.04	0.04
Max	5955.03	4867.80	8771.93	12700.77	63.43	4.00	5.00
Min	0.00	0.00	0.00	0.00	0.00	1.00	0.00
	Recruitment (trees∗ha^{-1}∗y^{-1})				z (km)	s (%)	α (°)
	Birch	Aspen	White spruce	Black spruce			
Mean	5.60	2.49	27.92	32.30	0.36	10.17	146.41
S.D.	0.97	0.69	2.63	6.48	0.01	0.60	5.09
Max	197.68	222.39	444.77	1161.35	0.96	77.00	360.00
Min	0.00	0.00	0.00	0.00	0.02	0.00	0.00

Table 4—Summary statistics for individual tree data

	Birch	Aspen	White spruce	Black spruce
		Diameter (cm)		
Mean	13.13	12.30	10.52	6.12
S.D.	7.57	6.03	7.23	3.90
Max	59.49	53.29	85.39	30.71
Min	3.80	3.80	3.80	3.80
n	6080	5206	11677	4862
		Diameter growth (cm∗y^{-1})		
Mean	0.10	0.08	0.11	0.09
S.D.	0.12	0.08	0.12	0.11
Max	1.55	0.81	2.50	1.82
Min	-3.99	-0.62	-2.27	-2.20
n	6080	5206	11677	4862
		Mortality Rate (y^{-1})		
Mean	0.02	0.03	0.01	0.01
S.D.	0.06	0.07	0.04	0.03
Max	0.20	0.20	0.20	0.20
Min	0.00	0.00	0.00	0.00
n	6885	6011	12161	5014

Table 5—Parameters of the recruitment equation

Explanatory Variables	Species							
	Birch		Aspen		White spruce		Black spruce	
Constant	-10278.00	**	3096.00		-5290.00		-511.00	
β_1	0.01	***	0.01	***	0.03	***	0.11	***
β_2	-0.36	***	-0.12	*	-0.68	***	-1.05	***
β_3	0.96		-900.30		1659.00		140.00	
β_4	3.09	**	1384.00		-7453.00		1030.00	
Spatial component								
d_1	2922.00	**	65.38		-129.00		-9.30	
d_2	3555.00		-324.70		49.00		-2703.00	
d_3	-207.66	**	-188.50		1036.20		-98.00	
d_4	-793.20		-0.91		6.66	**	-0.25	
d_5	-495.50		1.57	*	2.96		0.30	
Terrain component								
c_1	-0.17		-0.07		0.75		1.38	
c_2	-0.51		-0.02		0.14		0.15	
c_3	-0.11		-0.23		-0.75		-1.75	
c_4	1.04		-0.10		-4.78		-6.48	
c_5	4.10	**	0.50		-1.26		0.03	
c_6	0.40		0.71		4.26		8.02	
c_7	-0.91		0.08		3.15		2.52	
c_8	-3.62	**	-0.64		0.62		-1.66	
c_9	-0.13		-0.34		-3.65		-5.29	
c_{10}	3.28		-5.29		96.85	*	87.99	
c_{11}	-9.50		6.49		-127.59	**	-95.73	
R^2	0.19		0.19		0.35		0.79	
n	446		446		446		446	

Note:

-Dependent variable =stand recruitment in trees·ha^{-1}·y^{-1}.

-R^2= generalized coefficient of determination.

-*n* = degrees of freedom.

-Level of significance: *: P<0.10; **: P<0.05; ***: P<0.01.

-The complete model is:

$$R_i(\mathbf{s}) = \beta_0 + \beta_1 N(\mathbf{s}) + \beta_2 B(\mathbf{s}) + \beta_3 P(\mathbf{s}) + \beta_4 H(\mathbf{s}) + (d_1 x + d_2 y + d_3 x^2 + d_4 y^2 + d_5 x \cdot y)$$
$$+ l(\mathbf{s})[c_1 + c_2 \cos(\alpha(\mathbf{s})) + c_3 \sin(\alpha(\mathbf{s}))] + \ln(z(\mathbf{s}) + 1) \cdot l(\mathbf{s})[c_4 + c_5 \cos(\alpha(\mathbf{s})) + c_6 \sin(\alpha(\mathbf{s}))]$$
$$+ z(\mathbf{s})^2 \cdot l(\mathbf{s})[c_7 + c_8 \cos(\alpha(\mathbf{s})) + c_9 \sin(\alpha(\mathbf{s}))] + c_{10} z(\mathbf{s}) + c_{21} z(\mathbf{s})^2$$

Table 6—Percentage contribution (%) to the overall goodness-of-fit and the level of significance of variables and components

	Species							
	Birch		Aspen		White spruce		Black spruce	
	Recruitment (trees $ha^{-1} * y^{-1}$)							
Spatial component	3.56	***	6.23	**	8.77	***	2.53	*
Stem density	68.44	***	68.95	***	67.46	***	82.00	***
Stand basal area	6.32	***	1.69	*	2.73	***	4.88	***
Terrain component	8.02	***	8.77	*	16.21	***	8.41	*
Others (*P*, *H*)	13.67	**	14.35	*	4.83	*	2.20	
All	100.00	***	100.00	***	100.00	***	100.00	***
	Diameter Growth ($cm * y^{-1}$)							
Spatial component	10.18	***	4.30	***	12.28	***	24.89	***
Diameter	58.25	***	70.96	***	34.19	***	4.20	***
Stand basal area	13.97	***	5.38	***	10.72	***	4.60	***
Terrain component	12.45	***	13.80	***	17.85	***	32.59	***
Others (*P*, *H*)	5.14	***	5.55	***	24.96	***	33.71	***
All	100.00	***	100.00	***	100.00	***	100.00	***
	Mortality (y^{-1})							
Spatial component	25.32	*	13.48	***	32.62	***	12.26	***
Diameter	43.10	***	50.60	***	7.09	***	3.13	***
Stand basal area	1.70	***	8.27		7.30	***	2.22	
Terrain component	22.61	***	22.31	***	44.94	***	55.22	***
Others (*P*, *H*)	7.27		5.33	***	8.05	***	27.17	***
All	100.00	***	100.00	***	100.00	***	100.00	***

Note:

-Level of significance: *: $P<0.10$; **: $P<0.05$; ***: $P<0.01$.

-Due to the limit of computing capacity, percentage contribution (%) to the overall goodness-of-fit is approximated with the following terms by the hierarchical partitioning method:

$D, B, P, H, x, y, l, l \cdot \cos(\alpha), l \cdot \sin(\alpha), z, z^2$.

Table 7—Parameters of the diameter growth equation

	Species							
	Birch		Aspen		White spruce		Black spruce	
Constant	33.347	***	-40.126	***	-3.835		81.300	***
γ_1	0.022	***	0.017	***	0.014	***	0.014	***
γ_2	-0.754	***	-0.412	***	-0.381	***	-1.271	***
γ_3	8.457	***	4.236	***	3.242	***	28.367	***
γ_4	-0.003	***	-0.002		-0.003	***	0.000	
γ_5	0.006		0.004	**	0.032	***	0.027	***
γ_6	-0.003		-0.001	***	0.001		0.014	***
Spatial component								
d_1	-9.150	***	11.184	***	0.965		-22.802	***
d_2	-19.931	**	35.540	***	7.109	**	-38.110	***
d_3	0.628	***	-0.779	***	-0.060		1.598	***
d_4	3.992		-9.245	***	-5.985	***	9.880	***
d_5	2.704	**	-4.906	***	-0.888	**	5.167	**
Terrain component								
c_1	0.001	*	-0.001		-0.002	***	-0.002	
c_2	-0.001	***	0.002	***	-0.002	***	-0.003	**
c_3	0.002	**	0.000		0.001	**	-0.005	***
c_4	-0.014	***	0.012	***	0.007	***	-0.012	
c_5	0.003		-0.002		0.004	*	0.006	
c_6	-0.010	**	-0.009	**	-0.005	*	0.023	**
c_7	0.009		-0.014	***	-0.003		0.016	*
c_8	-0.002		-0.003		-0.004	*	0.000	
c_9	0.012	***	0.011	***	0.003		-0.016	*
c_{10}	0.180	***	-0.217	***	0.024		0.190	**
c_{11}	-0.241	***	0.275	***	-0.147	***	-0.255	**
R^2	0.16		0.30		0.19		0.09	
n	6079		5205		11676		4861	

Note:

-Dependent variable =diameter increment in $cm \cdot y^{-1}$.

-R^2= generalized coefficient of determination.

-*n* = degrees of freedom.

-Level of significance: *: $P<0.10$; **: $P<0.05$; ***: $P<0.01$.

-The complete model is:

$$g_{ij}(\mathbf{s}) = \gamma_0 + \gamma_1 D(\mathbf{s}) + \gamma_2 D^2(\mathbf{s}) + \gamma_3 D^3(\mathbf{s}) + \gamma_4 B(\mathbf{s}) + \gamma_5 P(\mathbf{s}) + \gamma_6 H(\mathbf{s}) + (d_1 x + d_2 y + d_3 x^2 + d_4 y^2 + d_5 x \cdot y)$$
$$+ l(\mathbf{s})[c_1 + c_2 \cos(\alpha(\mathbf{s})) + c_3 \sin(\alpha(\mathbf{s}))] + \ln(z(\mathbf{s}) + 1) \cdot l(\mathbf{s})[c_4 + c_5 \cos(\alpha(\mathbf{s})) + c_6 \sin(\alpha(\mathbf{s}))]$$
$$+ z(\mathbf{s})^2 \cdot l(\mathbf{s})[c_7 + c_8 \cos(\alpha(\mathbf{s})) + c_9 \sin(\alpha(\mathbf{s}))] + c_{10} z(\mathbf{s}) + c_{21} z(\mathbf{s})^2$$

Table 8—Parameters of the mortality equation

	Species							
	Birch		Aspen		White spruce		Black spruce	
Constant	-75.3843		-699.1010	***	-327.0340	**	-212.7930	
δ_1	-0.3089	***	-0.3942	***	-0.3292	***	0.1429	*
δ_2	0.0118	***	0.0142	***	0.0195	***	-0.0168	**
δ_3	-0.0001	***	-0.0002	***	-0.0003	***	0.0004	**
δ_4	0.0081	**	-0.0060		0.0161	***	-0.0121	
δ_5	0.0559		-0.3102	***	-0.1143	***	-0.3169	***
δ_6	-0.0109		0.0835	**	-0.0502		0.3124	***
Spatial component								
d_1	24.5381		203.0630	***	97.7920	**	75.7932	
d_2	-182.5720		-240.8970	**	-169.2840	**	-945.6830	**
d_3	-1.9537		-14.6711	***	-7.2783	**	-6.4794	
d_4	34.2778		-21.6544		91.0388	***	160.2830	*
d_5	25.2288		35.8469	***	21.7540	*	131.0860	**
Terrain component								
c_1	-0.0027		-0.0476	***	0.0032		0.0667	
c_2	0.0072		-0.0154		-0.0070		-0.0303	
c_3	0.0035		0.0121		0.0060		0.0983	**
c_4	0.2144	**	0.1727		0.0262		0.0651	
c_5	0.1074		-0.0983		0.0657		0.0834	
c_6	-0.0089		-0.1412		-0.2113	***	-0.7993	*
c_7	-0.4002	***	-0.0990		-0.0362		-0.4884	
c_8	-0.2906	**	0.0995		-0.0471		-0.3213	
c_9	0.0261		0.0699		0.2898	***	1.0591	*
c_{10}	-1.4572		-4.2703	***	-2.5270	***	-2.2706	
c_{11}	2.3799		2.4327		1.4191		-1.5049	
R^2	0.17		0.16		0.14		0.12	
n	6885		6011		12161		5014	

Note:

-Dependent variable =mortality rate in y^{-1}.

-R^2= McFadden's pseudo R-squared value.

-*n* = degrees of freedom.

-Level of significance: *: $P<0.10$; **: $P<0.05$; ***: $P<0.01$.

-The complete model was:

$$M_{ij}(\mathbf{s}) = \Phi(\delta_0 + \delta_1 D(\mathbf{s}) + \delta_2 D^2(\mathbf{s}) + \delta_3 D^3(\mathbf{s}) + \delta_4 B(\mathbf{s}) + \delta_5 P(\mathbf{s}) + \delta_6 H(\mathbf{s}) + (d_1 x + d_2 y + d_3 x^2 + d_4 y^2 + d_5 x \cdot y)$$
$$+ l(\mathbf{s})[c_1 + c_2 \cos(\alpha(\mathbf{s})) + c_3 \sin(\alpha(\mathbf{s}))] + \ln(z(\mathbf{s}) + 1) \cdot l(\mathbf{s})[c_4 + c_5 \cos(\alpha(\mathbf{s})) + c_6 \sin(\alpha(\mathbf{s}))]$$
$$+ z(\mathbf{s})^2 \cdot l(\mathbf{s})[c_7 + c_8 \cos(\alpha(\mathbf{s})) + c_9 \sin(\alpha(\mathbf{s}))] + c_{10} z(\mathbf{s}) + c_{21} z(\mathbf{s})^2$$

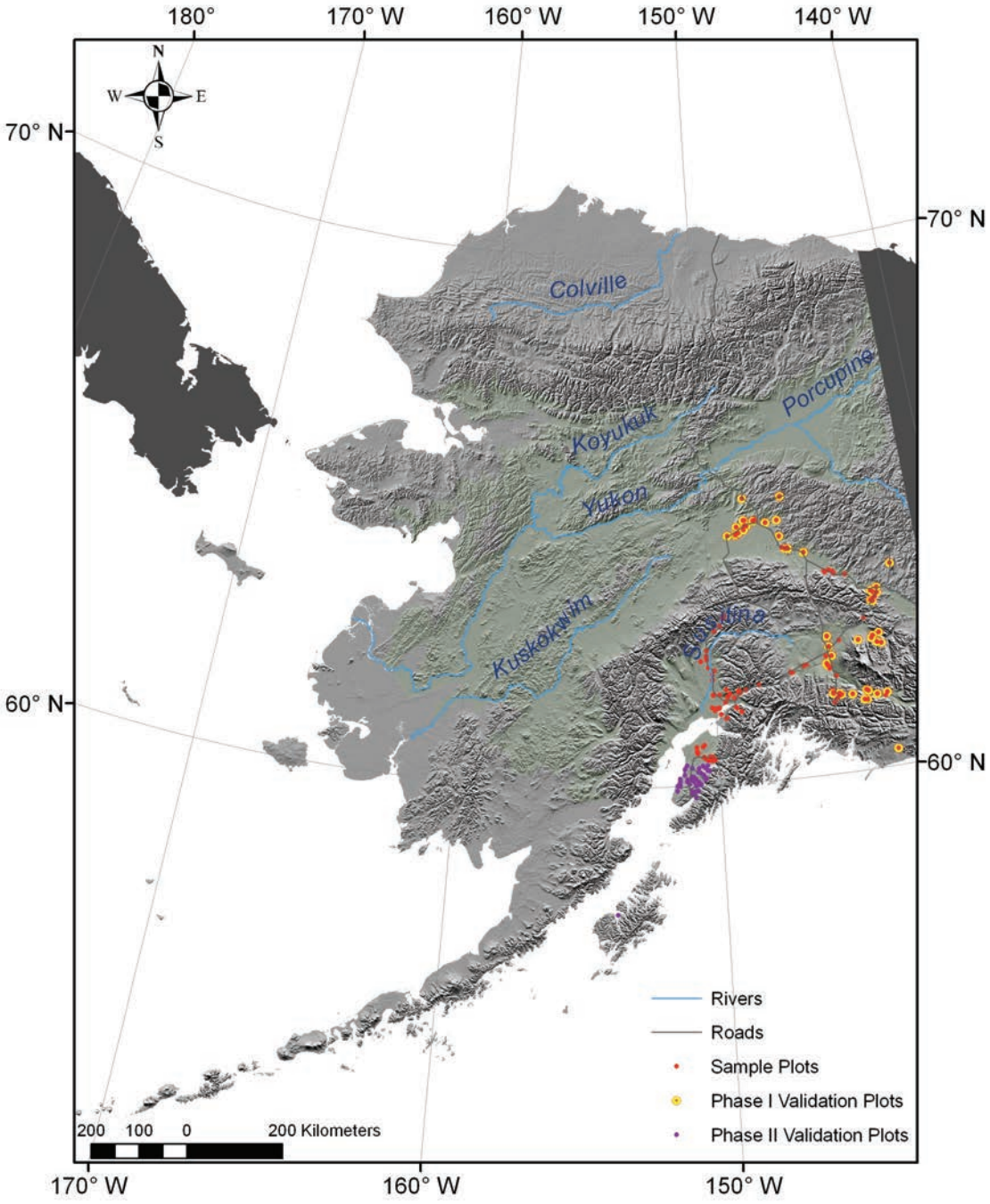

Figure 1—Geographic distribution of the sample and validation plots and their relative location in the Alaska boreal forest region (green area. Source: the U.S. Geological Survey Ecoregions Map of Alaska, http://agdc.usgs.gov/data/projects/fhm/). Albers equal area map projection with standard parallels.

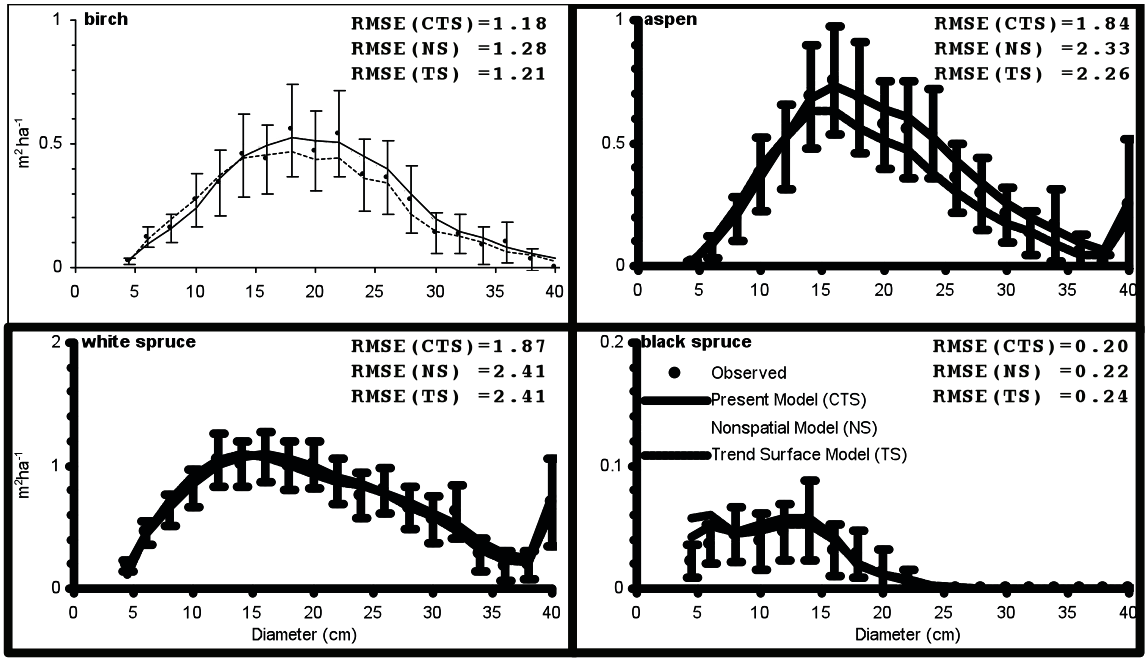

Figure 2—Average predicted and observed basal area by diameter class and species with 95 percent confidence interval over the 175 Phase I validation plots. Predictions were obtained with the present model (1), the nonspatial model (2), and the uncontrolled trend surface model (3). RMSE represents root mean squared errors calculated for that species by the three different models.

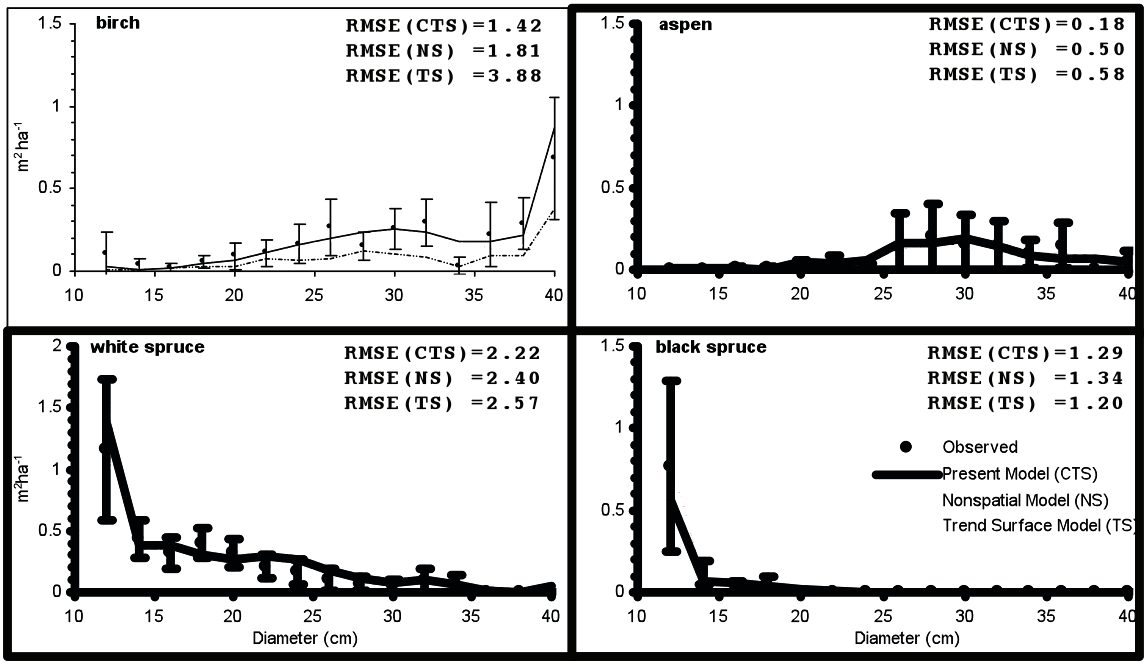

Figure 3—Average predicted and observed basal area by diameter class and species over the 40 Phase II validation plots. Vertical bars represented 90 instead of 95 percent confidence interval of observed values due to the small number of plots. Predictions were obtained with the present model (CTS), the nonspatial model (NS), and the conventional trend surface model (TS). RMSE represents root mean squared errors calculated for that species by the three different models.

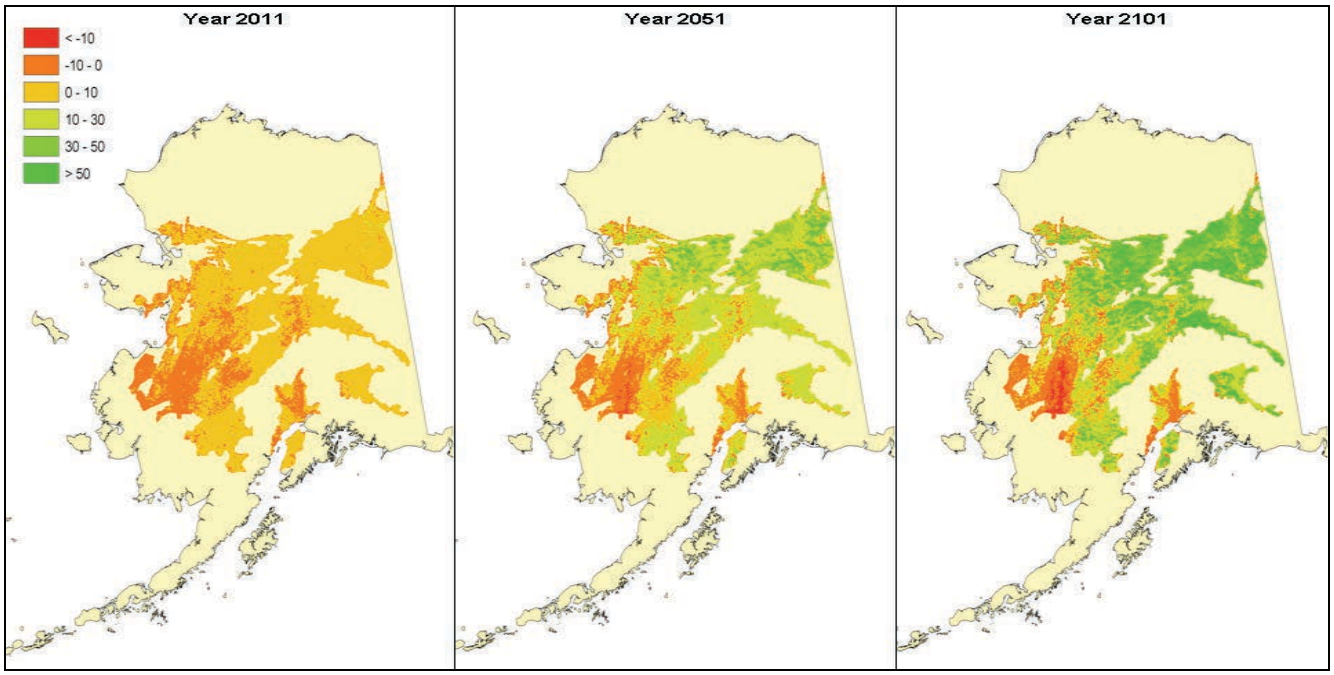

Figure 4—Predicted stand basal area change (m^2ha^{-1}) of the Alaska boreal forest in the year 2011, 2051, and 2101, assuming constant climate conditions and no major natural disturbances. The initial stand states were obtained from the 2001 NLCD Landsat remote sensing data.

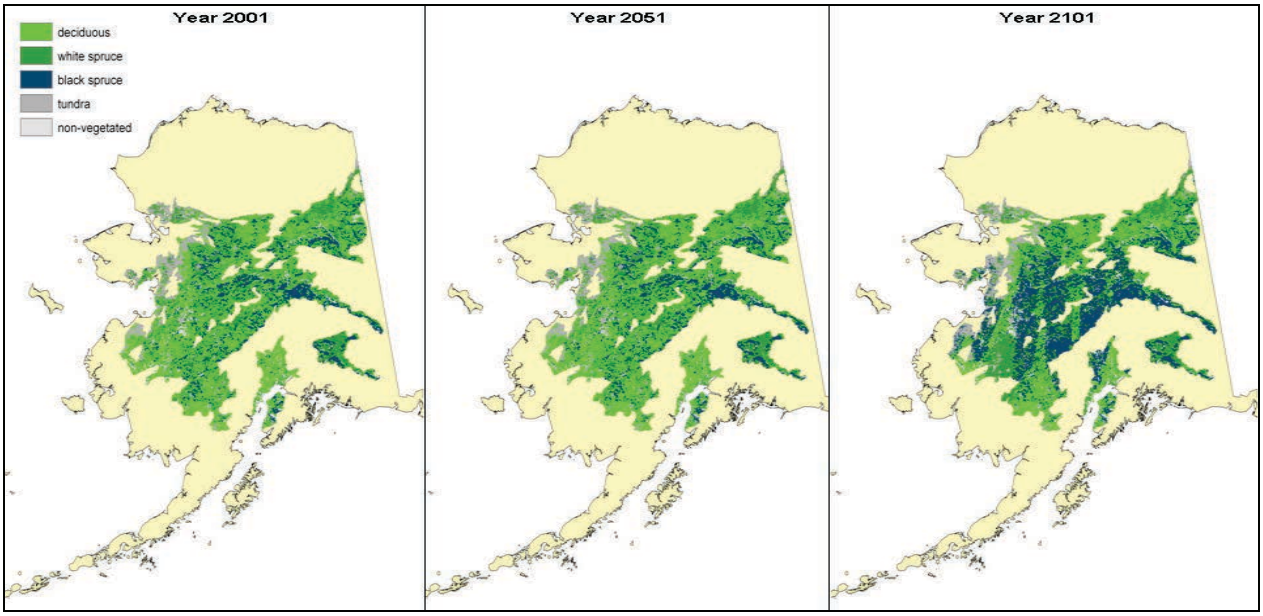

Figure 5—Observed (year 2001) and predicted (year 2051 and 2102) tree species coverage in the boreal forest region of Alaska, assuming constant climate conditions and no major natural disturbances. The initial stand states were obtained from the 2001 NLCD Landsat remote sensing data.